

## Multiple bonding configurations for Te adsorbed on the Ge(001) surface

P. F. Lyman

*Department of Materials Science and Engineering and Materials Research Center, Northwestern University, Evanston, Illinois 60208  
and Department of Physics, University of Wisconsin-Milwaukee, Milwaukee, Wisconsin 53201*

D. L. Marasco and D. A. Walko

*Department of Materials Science and Engineering and Materials Research Center, Northwestern University, Evanston, Illinois 60208*

M. J. Bedzyk\*

*Department of Materials Science and Engineering and Materials Research Center, Northwestern University, Evanston, Illinois 60208  
and Materials Science Division, Argonne National Laboratory, Argonne, Illinois 60439*

(Received 22 January 1999)

Using high-resolution x-ray standing waves and low-energy electron diffraction, the structure of Te adsorbed on Ge(001) was studied. A coverage-dependent structural rearrangement was observed between Te coverages of 1 and 0.5 monolayer (ML). At Te coverages near 1 ML, Te was found to adsorb in a bridge site, as expected. However, at Te coverages near 0.5 ML, a structure unanticipated for Group VI/Group IV adsorption was discovered. Te-Ge heterodimers were formed with an average valency of 5, allowing them to satisfy all surface dangling bonds. The results help explain the efficacy of Te as a surfactant in epitaxial growth of Ge/Si(001). [S0163-1829(99)08635-X]

### I. INTRODUCTION

The clean surface of a semiconductor is generally reactive and reconstructed. Often, a clean surface may be passivated by the adsorption of a monolayer of a foreign species with certain chemical characteristics. The surface will be chemically passivated if this adsorption leads to a reduction in reactivity of the surface, and/or may be electronically passivated if electronic states induced by the surface truncation are removed or quenched.

The passivated surface will have a lower surface energy than the clean surface, which can have profound effects on the properties of the surface system. For instance, the phenomenon of surfactant-mediated epitaxy (SME) depends critically on this lowering of the surface energy.<sup>1</sup> Briefly, SME refers to the segregation of the foreign species (the “surfactant”) to the vacuum interface when another material is deposited on top of the surfactant-terminated surface. The segregation, which is driven by the system’s propensity to maintain a low surface energy, can dramatically alter the kinetics of subsequent epitaxial growth.<sup>2</sup> The presence of the surfactant can delay the onset of three-dimensional islanding<sup>3</sup> for systems that grow in the Stranski-Krastanov mode, or can even allow the construction of thermodynamically unstable alloys.<sup>4</sup>

The present paper focuses on the passivation of the (001) face of a Group-IV semiconductor [Ge(001)] with a Group-VI adsorbate (Te). The motivation for studying the structure of this adsorption system can be understood by briefly examining the valency and arrangement of the adsorbate and surface layer. The unreconstructed (001) face of a diamond-structure semiconductor has two dangling bonds per surface atom. Therefore, the adsorption of 1 monolayer (ML) of a hexavalent Group-VI element could saturate all available surface bonds, resulting in a perfect (1×1) termination. This adsorbate-induced dereconstruction has previ-

ously been demonstrated for S/Ge(001),<sup>5</sup> and, somewhat imperfectly, for Te/Si(001);<sup>6</sup> in each case, the Group-VI element was found to adsorb in a bridge site.<sup>7</sup>

The SME of Ge on Si(001) using Te as a surfactant,<sup>8–12</sup> however, has raised additional questions about both the mechanism of the surfactant action and the structure of Te on Si(001) and Ge(001). Surprisingly, Te was able to act as an effective surfactant for that system down to a Te coverage of only 0.1 ML.<sup>10</sup> This is somewhat difficult to explain since passivation of the surface should require termination by a full adsorbate ML. Moreover, after prolonged Ge growth, an unexplained surface symmetry [ $c(2\times 2)$ ] was reported.<sup>9,11,12</sup> It was not clear in these SME studies whether that new superstructure was due to the altered chemical identity of the new “substrate” (i.e., Ge), or whether the strained surface<sup>13</sup> played a dominant role.

To resolve these issues and to investigate passivation of Ge, we conducted a detailed structural study of Te adsorption on a native Ge(001) surface using x-ray standing waves (XSW) and low-energy electron diffraction (LEED). As expected, we found that a full ML of Te could passivate the Ge(001) surface by adsorbing in bridge sites with a predominantly (1×1)-like local arrangement. In addition, however, we found a coverage-dependent transition to a  $c(2\times 2)$  superstructure, accompanied by a dramatic shift in Te adsorption position. We explain these findings with a model where Te-Ge dimers are formed, with an ideal Te coverage of 0.5 ML. This structure is also able to satisfy all surface dangling bonds, despite the reduced Te coverage. We argue that this previously unreported structure can explain both the appearance of  $c(2\times 2)$  LEED spots and the low-coverage surfactant action during SME of Te/Ge/Si(001).

### II. EXPERIMENT

The experiments were conducted at beamline X15A of the National Synchrotron Light Source at Brookhaven National

Laboratory. The apparatus consisted of several coupled ultrahigh vacuum (UHV) chambers (base pressure  $\sim 9 \times 10^{-11}$  torr) allowing sample preparation (molecular-beam epitaxial growth) and characterization [LEED, Auger electron spectroscopy (AES), and XSW]. The XSW technique and the experimental arrangement at X15A have been extensively reviewed by Zegenhagen.<sup>14</sup> A simple video camera was used to digitize the LEED images shown here.

The Ge(001) samples were polished and degassed *ex situ*, and were then mounted in a strain-free manner on a molybdenum holder prior to insertion into UHV. After degassing, each sample was sputtered for 1 h at  $T_{\text{sub}} \approx 500$  °C using 500-eV Ar<sup>+</sup> ions. Each was then annealed for 10 min at 690 °C, and then slowly cooled to room temperature (initial cooling rate  $\approx 2.0$  °C/s). The annealing temperature used is below the Ge roughening temperature, and should result in greater long-range order.<sup>15</sup> This cycle was repeated several times, resulting in a sharp, two-domain ( $2 \times 1$ ) LEED pattern with clear  $c(4 \times 2)$  streaks. AES could detect no O and typically a small amount of C contamination ( $\sim 0.01$  ML).

Te was deposited from an effusion cell at  $\approx 0.25$  ML/min (1 ML =  $6.25 \times 10^{14}$  cm<sup>-2</sup>) on the single-crystal Ge(001) substrates held at  $T_{\text{sub}} \approx 270$  °C. Samples were prepared to a saturation coverage by exposure to  $\sim 3$  ML of Te. After LEED and AES investigation, the samples were analyzed by XSW. In addition, another surface condition was investigated by AES, LEED, and XSW after further annealing to  $T_{\text{sub}} = 420$  °C for 10 min. We found that annealing to  $T_{\text{sub}} = 550$  °C resulted in complete desorption of the Te layer. After removing the sample from the vacuum chamber, the Te coverage was determined by comparing the intensity of the Te *L* fluorescence to the *L* fluorescence of an In-implanted sample whose areal In density had been previously calibrated by Rutherford backscattering spectrometry.

For XSW analysis, the incident x-ray beam from the synchrotron radiation source was collimated and monochromated by a double-crystal monochromator and directed through a Be window into the UHV chamber. The sample was held at room temperature and placed so that the x-ray beam was Bragg reflected by either the (004) or the (022) set of diffraction planes, using 7.5 and 7.1-keV x-rays, respectively. Angular piezoelectric drives on both monochromator crystals were used to precisely scan through the several arcseconds-wide Bragg reflection. At each angular step in the scan, an x-ray fluorescence spectrum was collected from an energy-dispersive Si(Li) detector and the reflected x-ray beam was measured by an *in vacuo* Si photodiode.

### III. RESULTS

#### A. 1 ML Te/Ge(001)

After saturation with Te at 270 °C, the Te coverage was found using x-ray fluorescence to be  $1.0 \pm 0.1$  ML.<sup>16</sup> In addition, a distinctive, streaky LEED pattern was observed (Fig. 1). It is evident that significant intensity extends from the (00) spot to the {10} spots, and also at the zone edge from the {10} spots to the {11} spots. This streaked intensity reveals a disordering along one crystallographic direction, with sharp ordering in the perpendicular direction, as will be discussed below.

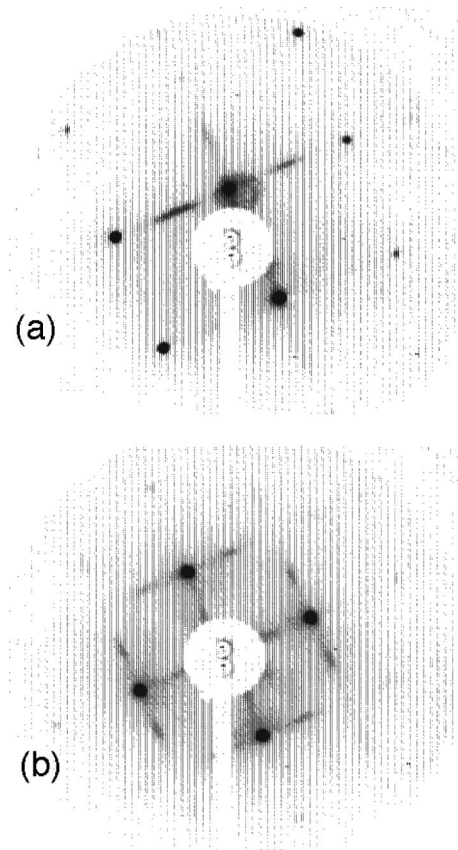


FIG. 1. LEED patterns for Te adsorbed on Ge(001) at 270 °C acquired at room temperature (RT) at (a) 49 eV and (b) 68 eV [streaky ( $1 \times 1$ ).]

To our knowledge, only one LEED pattern has previously been reported for this adsorption system.<sup>9</sup> The pattern was not discussed in detail, but was reported to be a streaky ( $1 \times 1$ ), similar to Fig. 1. It is also worth considering more extensive studies of two similar cases, those of S/Ge(001) and Te/Si(001). Deposition of atomic S on Ge(001) resulted in a sharp ( $1 \times 1$ ) LEED pattern.<sup>5</sup> In that study, x-ray photoelectron spectroscopy results supported a local arrangement where S atoms were adsorbed at bridge sites. Taken together, these results imply a well-ordered ( $1 \times 1$ ) structure exists for S/Ge(001). However, a streaky pattern, somewhat similar to the present one for Te/Ge(001), has been observed for Te/Si(001)<sup>6,8,9,17,18</sup> for preparation conditions like the ones used here,<sup>19</sup> and we have reproduced this pattern for Te/Si(001).<sup>20</sup> This pattern has been described as a “streaky ( $1 \times 1$ ).”<sup>6,8,9</sup> Indeed, the pattern arising from our Te/Si(001) surface has streaks of intensity that extend all the way from the (00) spot to the four {01} spots.<sup>20</sup> This pattern had been interpreted as arising from a local ( $1 \times 1$ ) geometry [as for S/Ge(001)], but with a random distribution of missing Te rows.<sup>6</sup> Scanning, tunneling microscopy (STM) images clearly revealed that large areas having ( $1 \times 1$ ) local structure were interrupted by long atomic rows devoid of Te.<sup>6</sup>

In the present Te/Ge(001) pattern, however, it is clear that the intensity along the (00)-{01} directions is broadly peaked at the half-order spot, i.e., near  $\{0\frac{1}{2}\}$  positions. In addition, this pattern shows intensity extending from the {11} to {01} spots, which was not reported in the Te/Si(001) case. After

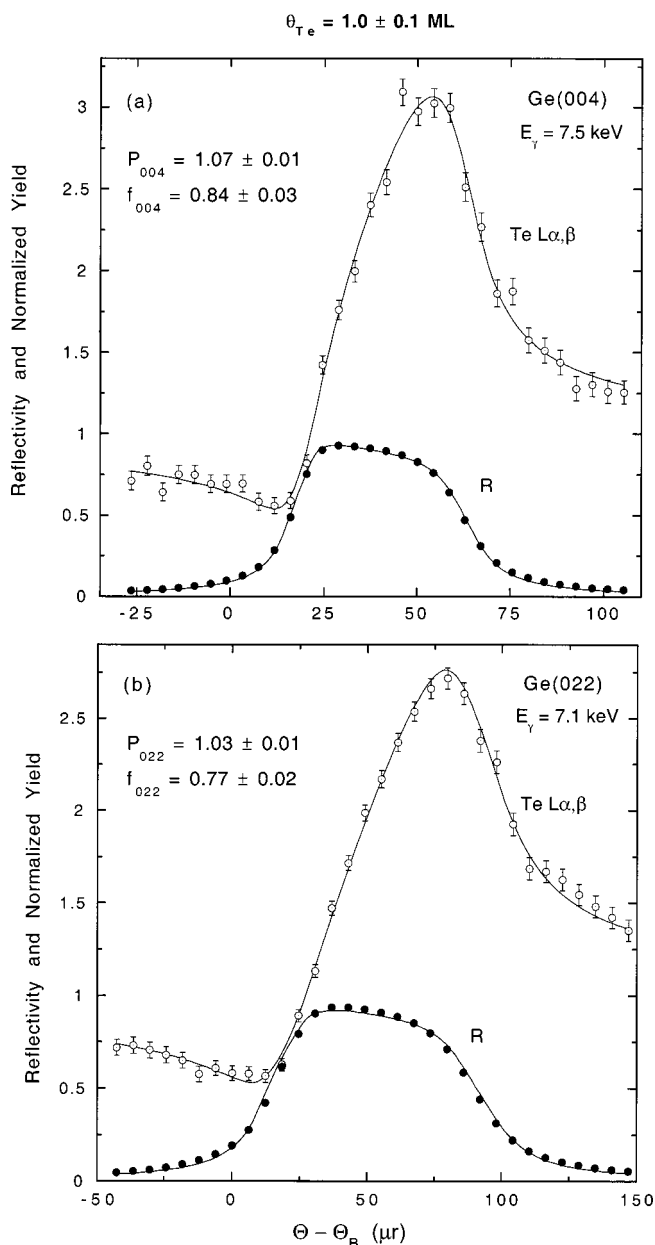


FIG. 2. XSW scan for the (a) (004) and (b) (022) diffraction planes for Te/Ge(001) sample annealed to 270 °C. Te coverage is  $\approx 1$  ML.

this observation, a more careful measurement of our Te/Si(001) patterns revealed that the intensity is also peaked at the half-order positions on that surface, although the peak is much less pronounced.<sup>20</sup> There is also a small amount of intensity in that case at the sides of the zone, from the  $\{11\}$  to  $\{01\}$  spots. In light of these observations, we will refer to the Te/Ge(001) pattern in Fig. 1 as a “streaky  $(1 \times 1)$ ,” but note that there is a weak peak of intensity at the half-order positions.

The results from an XSW measurement using the (004) diffraction vector for this surface preparation are shown in Fig. 2(a). The strong modulation seen in the Te fluorescence signal is indicative of a highly uniform Te atom distribution. Indeed, the best fit [solid line in Fig. 2(a)] reveals a coherent fraction  $F_{004}$  of  $0.84 \pm 0.03$ . This value clearly indicates that only one atomic position [with respect to the (004) planes] is

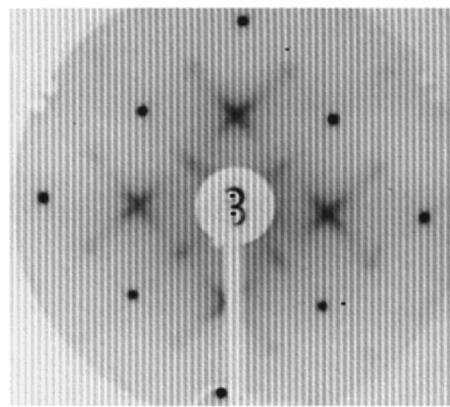


FIG. 3. LEED pattern for a Te/Ge(001) sample annealed to 420 °C acquired at RT at 44 eV. [Streaky  $(\sqrt{2} \times \sqrt{2})R45^\circ$ .]

occupied. We expect the Te mean-square-displacement normal to the surface  $\langle u_{004}^2 \rangle^{1/2}$  to be approximately  $0.13 \pm 0.015$  Å.<sup>21</sup> This vibrational motion should lead to a Debye-Waller reduction in the coherent fraction by a factor of  $0.85 \pm 0.03$ . Thus, all of the width of the Te atom distribution along (004) can be accounted for by thermal vibrations.

The measured coherent position  $P_{004}$  was found to be  $1.07 \pm 0.01$ , which corresponds to an adsorption height above the bulk-extrapolated (004) surface plane of  $1.52 \pm 0.02$  Å. This position is consistent with adsorption in a bridge site. If the top Ge atoms are in relaxed, bulklike positions,<sup>22</sup> this would imply a Te-Ge bond length of approximately  $2.56 \pm 0.03$  Å, compared to the sum of Pauling tetrahedral atomic radii of 2.54 Å.<sup>23</sup> Another estimate of bond lengths of covalently bonded Te-Ge compounds with similar coordinations comes from electron diffraction<sup>24</sup> and extended x-ray absorption fine structure<sup>25,26</sup> studies of amorphous TeGe compounds, which found Ge-Te distances of 2.59–2.605 Å.

An XSW measurement was also performed using the (022) Bragg reflection for this surface preparation. [See Fig. 2(b).] (Note that the expected two rotational domains on the Ge(001) surface are equivalent with respect to this diffraction vector.) The coherent position  $P_{022}$  was found to be  $1.03 \pm 0.01$ . For an atomic spatial distribution that is centered about a twofold symmetry site,  $P_{022}$  is equivalent to  $\frac{1}{2}(1 + P_{004})$ . This condition is satisfied for the present measurements. The measured coherent fraction  $F_{022}$  is  $0.77 \pm 0.02$ . This value is slightly reduced compared to the (004) case, as will be discussed below.

### B. $\frac{1}{2}$ ML Te/Ge(001)

After annealing the sample to 420 °C for 10 min, a dramatic change in the LEED pattern was observed. (See Fig. 3.) The predominant feature became a crosslike pattern of intensity located at the  $\{\frac{1}{2}, \frac{1}{2}\}$  positions. In addition, some weak spots of intensity were observed at the  $\{0, \frac{1}{2}\}$  and  $\{1, \frac{1}{2}\}$  positions, reminiscent of the clean surface pattern. This LEED pattern has never been reported for Te/Ge(001) before, but a similar pattern has repeatedly been observed during surfactant-mediated growth of Ge/Si(001) with Te as the surfactant.<sup>9,11,12</sup> Its origin is unknown, but the simplest interpretation of this pattern is that two rotational domains of a

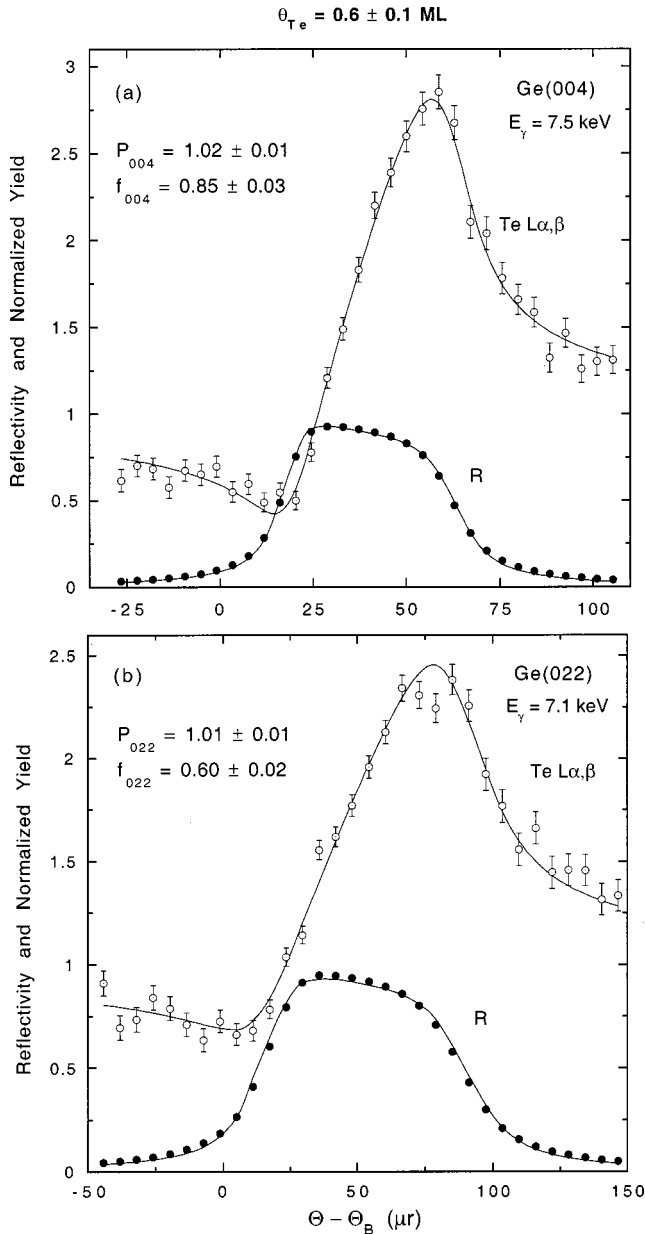


FIG. 4. XSW scan for the (a) (004) and (b) (022) diffraction planes for a Te/Ge(001) sample annealed to 420 °C. Te coverage is  $\approx 0.6$  ML.

streaky  $c(2 \times 2)$  pattern [more properly a “streaky  $(\sqrt{2} \times \sqrt{2})R45^\circ$ ” pattern] coexist with a  $(2 \times 1)$  pattern. Presumably, the Te are arranged in small domains with  $(\sqrt{2} \times \sqrt{2})R45^\circ$  local geometry, and there are also areas, either Te-covered or of bare Ge, having a  $(2 \times 1)$  reconstruction. The (Te *MNN*)/(Ge *LMM*) Auger ratio was found to decrease upon annealing to 0.6 that of the low-temperature surface, indicating significant desorption of Te occurred. We did not perform fluorescence analysis on this sample, but estimate the coverage to be  $0.6 \pm 0.1$  ML based on the AES and fluorescence results from the low-temperature structure. As mentioned above, all of the Te desorbed from the sample upon annealing to 550 °C.

The (004) XSW data and analysis are shown in Fig. 4(a). The measured coherent position  $P_{004}$  was found to be  $1.02 \pm 0.01$ , indicating a Te-adsorption height above the bulk-

extrapolated (004) surface plane of  $1.44 \pm 0.02$  Å. This value represents an inward shift of 0.08 Å compared to the surface prepared with the lower annealing temperature. A high coherent fraction  $F_{004}$  of  $0.85 \pm 0.03$  was found, indicating that only one atomic adsorption position [with respect to the (004)-planes] is occupied. Due to this inward shift and the change in the surface long-range order, it is unlikely that the high-temperature position can be explained by adsorption in a simple bridge site. A Te adsorbate in a bridge site at the measured adsorption height would have a Te-Ge bond length of approximately 2.48 Å, significantly smaller than the sum of the tetrahedral covalent radii.

For the (022) measurement, the coherent position  $P_{022}$  of  $1.01 \pm 0.01$  is again consistent with the result expected (from the  $P_{004}$  value) for a symmetric atomic spatial distribution. [See Fig. 4(b).] However, the measured coherent fraction  $F_{022}$  of  $0.60 \pm 0.02$  is significantly lower than  $F_{004}$ . This value indicates that more than one inequivalent atomic position [with respect to the (022) planes] is occupied. This observation also argues against occupation of a bridge site: since the bridge site is located directly at a twofold symmetric site, a population composed of bridge-site atoms will necessarily contain only positions that are equivalent with respect to the (022) planes. Thus, we conclude that, upon heating to 420 °C, the surface undergoes a structural transition wherein approximately half the Te is desorbed, and the remaining Te atoms occupy a fundamentally different atomic site.

## IV. DISCUSSION

### A. 1 ML Te/Ge(001) structure

The low-temperature-annealed (1 ML Te) structural data are natural to interpret in terms of the simple bridge-bonded position that is suggested from simple valency considerations, and appears in the related S/Ge(001) (Ref. 5) and Te/Si(001) systems.<sup>6,7</sup> There is also some experimental<sup>27</sup> and theoretical<sup>28–30</sup> evidence that this site is occupied in the Se/Si(001) system, and also some experimental<sup>31</sup> and theoretical<sup>29</sup> support for this site for S/Si(001).

Indeed, the present XSW data for the low-temperature structure strongly favor the simple bridge-bonded configuration. However, the LEED pattern is streaked, i.e., there are  $\{0 \frac{1}{2}\}$  spots that are greatly elongated along one direction, but are fairly sharp in the transverse direction. These observations favor a model that has good long-range order in one direction but significant disorder in the other direction. The slight peaking at the half-order position reveals the existence of a weak  $(2 \times 1)$  periodicity in the long-range order that is not easily explained by this local structural model.

In an incisive STM study of Te/Si(001), large regions of  $(1 \times 1)$  local structure were seen to be irregularly interrupted by long rows devoid of adsorbates, with an average width for the Te-occupied regions of 5 to 6 rows.<sup>6</sup> The origin of the missing rows is thought to be the compressive surface stress induced by placing larger-atomic-radius Te adsorbates on the Si substrate. This stress must be relieved by occasional missing Te rows, reducing the Te coverage to approximately 0.75–0.83 ML.<sup>6,12</sup> The missing row of Te allows the Te islands to expand laterally, so that adjacent Te islands were

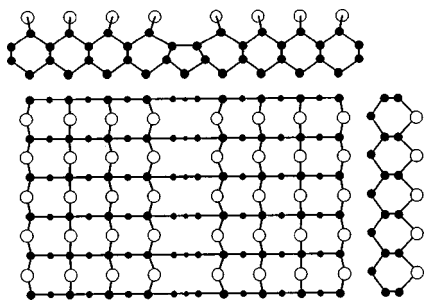


FIG. 5. Schematic diagram of the Te/Ge(001)-(1 $\times$ 1) structure. The Te atoms (open circles) are in bridge positions. A missing Te and Ge row is shown, allowing lateral Te relaxation. (Note the different crystallographic orientation of the missing Te row than Fig. 6 of Ref. 6.)

separated by only approximately  $1.5a$  [ $a = 3.84 \text{ \AA}$ , the Si(001) unit cell dimension].<sup>6</sup> (See Fig. 5.) Stress-relieving arrays of missing adsorbate rows have also been observed in the Sb/Si(001) (Ref. 32) and Bi/Si(001) (Ref. 33) systems. As mentioned above, the random array of missing rows for Te/Si(001) can explain the streaking in the (1 $\times$ 1) LEED pattern. (It cannot, however, explain any peaking of intensity at the half-order positions.) Further, note that no streaking was reported for the S/Ge(001)-(1 $\times$ 1) case,<sup>5</sup> where the atomic radii of S and Ge would not suggest that the surface is under compressive stress.

For the present case of Te/Ge(001), the similarity of the LEED patterns to those for Te/Si(001) described in the literature<sup>6,8,9,17,18</sup> and observed in our laboratory<sup>20</sup> leads us to believe that similar mechanisms are at work. Although the Ge lattice is 4.3% larger than that of Si, it is still likely that the Ge surface cannot accommodate a full ML of Te adsorbates. While the central value of our absolute measurements of the saturation Te coverage is 1.0 ML, these considerations make it more likely that the true value lies at the lower side of the uncertainty ( $\pm 0.1$  ML). Thus, missing Te rows are also expected for Te/Ge(001), accounting for the streaking observed in the present studies. Moreover, the lateral expansion of the Te islands would place the Te atoms in slightly inequivalent positions with respect to the (022) [but not the (004)] diffraction vector. In the Te/Si(001) case, the average Te-Te distance was approximately  $4.1 - 4.2 \text{ \AA}$ .<sup>6</sup> If this Te-Te spacing is maintained for the Te/Ge(001) surface, then an average width for the Te-occupied regions of approximately 8 rows would fully account for the observed reduction of the coherent fraction  $F_{022}$  to  $0.77 \pm 0.02$ . The increased separation between missing rows for Ge compared to Si is also in agreement with the lower compressive surface stress expected for Ge (due to its larger lattice spacing), and the Te coverage predicted by this model is consistent with our measured value.

It is not possible with the present data alone to explain the origin of the weak (2 $\times$ 1) periodicity observed with LEED. However, combining the results of this study with previously published work for Te/Si(001), it is possible to construct a model consistent with the observed data. The  $\{0\frac{1}{2}\}$  LEED beams were elongated in the (00)-{01} direction, but sharp in the transverse (i.e.,  $\{\bar{1}\frac{1}{2}\}-\{1\frac{1}{2}\}$ ) direction. This result indicates that there is good long-range order in one direction, and

poor long-range order in the other direction; furthermore, the direction of good long-range order must be perpendicular to the direction of the doubling of the unit-cell periodicity.

In the STM study of missing rows of Te in the Te/Si(001) system, the last occupied Te rows were observed to expand laterally into the missing row. We suggest that the pairing responsible of the (2 $\times$ 1) LEED pattern occurs within the missing row. However, the direction of the unit-cell-doubling precludes a simple dimerization of Ge left uncovered by Te, as that dimerization would necessarily be parallel to the missing row. Instead, we suggest that an atomic row of Ge is also missing. This arrangement would allow the Te rows to expand laterally without stretching the length of the Te-Ge bonds, consistent with relieving the stress resulting from adsorbing large Te atoms into the Ge lattice. The unsaturated Ge atoms would then rebond across the missing row, reminiscent of a surface dimer, to lower their dangling bond density, as schematically indicated in Fig. 5.

Since the missing rows are expected to have an average spacing of about 8 times the Te row spacing, several missing-row structures would be found within the coherence length of the LEED beam. This atomic arrangement would lead to a (1 $\times$ 2) diffraction spot that was sharp in one direction (since the rows are long) but elongated in the other direction (since the rows are only one dimerized-unit wide with a broad distribution of row-row spacings),<sup>34</sup> consistent with the observed diffraction pattern. We caution that we have no direct evidence for the Ge bonding arrangement shown in Fig. 5, but note that this is a common distortion of the diamond lattice found at defects at *internal* interfaces as a way of accommodating stress.<sup>35</sup> It seems likely that similar configurations could be found in the selvedge region in response to adsorbate-induced stress. Note that the STM study<sup>6</sup> found that annealing to 300  $^{\circ}\text{C}$  in the presence of as little as 0.1 ML Te was sufficient to cause ML-deep "trenches" to form in the Si substrate, suggesting that Te is easily capable of inducing the suggested rearrangement in Ge.

In contrast to this model that requires submonolayer Te coverage, it is worth examining a careful LEED study<sup>18</sup> of (1 $\times$ 2) periodicity in the related case of Te/Si(001). After annealing to 600  $^{\circ}\text{C}$ , the (1 $\times$ 1) pattern for Te/Si(001) was seen to give way to a sharp (1 $\times$ 2) pattern. This transition was characterized by streaky splitting of the nascent half-order spots during annealing above 400  $^{\circ}\text{C}$  before the intensity coalesced into a well-defined (1 $\times$ 2) spot at 600–650  $^{\circ}\text{C}$ . The streaking was interpreted as stemming from spreading of (1 $\times$ 2)-like domain walls separating regions of (1 $\times$ 1) local structure; eventually, the (1 $\times$ 2) domains cover the whole surface. No claims were made for the atomic geometry accounting for the (1 $\times$ 2) structure. However, it was inferred that the local Te coverage was still 1 ML, and that some unexplained pairing of Te atoms was responsible for the (1 $\times$ 2) periodicity. This picture was supported by a "preliminary tensor LEED analysis,"<sup>18</sup> but was not followed up in a subsequent publication.<sup>17</sup>

Similarly, Te-Te dimers were proposed in a different study to explain a sharp (1 $\times$ 2) pattern reported for Te/Si(001).<sup>36</sup> In that work, however, Te was deposited by exposing the substrate to a CdTe flux as it cooled from 850  $^{\circ}\text{C}$  to 350  $^{\circ}\text{C}$  the high-temperature exposure reportedly

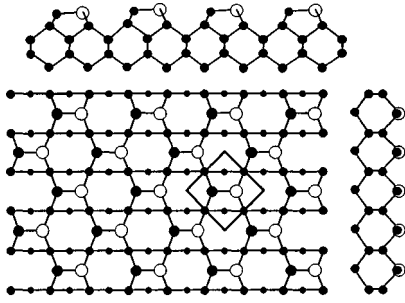


FIG. 6. Schematic diagram of the Te/Ge(001)- $(\sqrt{2}\times\sqrt{2})R45^\circ$  structure. Te and Ge atoms form dimers, which are located on the indicated  $(\sqrt{2}\times\sqrt{2})R45^\circ$  mesh.

resulted in significant Te indiffusion.<sup>36</sup> High-temperature CdTe exposure has even been reported to produce a SiTe<sub>2</sub> structure at the CdTe/Si(001) interface.<sup>37</sup> Thus, it is not clear that this surface is related to one formed by low-temperature exposure to elemental Te. Moreover, it is difficult to explain what the driving force for Te-Te dimer formation would be. In summary, we cannot rule out the possibility that such Te-Te pairing is responsible for the  $(1\times 2)$  periodicity evident for Te/Ge(001), and acknowledge that such pairing could also explain the small diminution in the value of  $F_{022}$  recorded for this surface. However, we argue that the missing-row scenario more simply explains the observations, is better justified by valency considerations, and has been more conclusively demonstrated via STM for the case of Te/Si(001).

### B. $\frac{1}{2}$ ML Te/Ge(001) structure

The high-temperature-annealed structure is more elusive to determine than the low-temperature structure. Since the AES signal is about 0.6 that of the low-temperature case, the Te coverage is consistent with 0.5 ML ( $0.6\pm 0.1$  ML). The inward shift of the Te atoms compared to the low-temperature structure means that the high-temperature structure cannot simply consist of a different long-range ordering of the same local Te structure, i.e., the XSW data rule out simple-bridge occupancy.

Turning back to valency considerations, we observe that it is possible to satisfy all dangling bonds with only one Te atom for every two surface unit cells. We propose that a Te-Ge dimer spans each pair of surface unit cells. With the arrangement of heterodimers shown in Fig. 6, this can form a  $(\sqrt{2}\times\sqrt{2})R45^\circ$  superstructure unit cell, easily and naturally explaining the symmetry of the LEED pattern observed.

The consistency of this proposed structure with valency requirements can be most easily shown by the following thought experiment. Consider a Ge(001) surface covered with Group-V atoms [As,<sup>38</sup> Sb,<sup>39</sup> or Bi (Ref. 4)]. In those known structures, a dimer for each two unit cells fills all dangling bonds of both the surface Ge layer and the Group-V layer. The Group-V atoms have one filled lone-pair orbital plus three covalent bonds. (Simple electron counting would result in  $2e/\text{lone pair}+3e/\text{covalent bonds}=5$  valence electrons per atom.) Now imagine, in the classic way,<sup>40</sup> transporting one proton from one member of the Group-V dimer to the other member, resulting in a heterodimer composed of one Group-IV atom and one Group-VI atom. Again, the av-

erage valency of the surface adsorbates is 5, and again this arrangement can satisfy all substrate dangling bonds as well as obey electron counting. This model implies some charge is transferred from the Group-VI element to the Group-IV element.

The LEED pattern displayed in Fig. 3 is not a sharp  $(\sqrt{2}\times\sqrt{2})R45^\circ$ , as the local structural model of Fig. 6 would predict. We attribute the streaking of the  $\{\frac{1}{2}\frac{1}{2}\}$  spots to antiphase domains across the reconstructed surface. As discussed in more detail below, the photoemission results of Bennett *et al.* for Te/Ge/Si(001)- $(2\times 2)$  revealed only Ge bound to 0 or 1 Te atom.<sup>12</sup> Thus, the heterodimers in a given domain must be predominantly oriented in one direction, as indicated in Fig. 6, or else Ge coordinated to 2 Te atoms would occur in significant numbers. It is, however, likely that the energy barrier associated with orientational antiphase domains would be quite small, since it is possible to create such an antiphase domain boundary merely by having some 2-Te-coordinated Ge atoms at the edge of the domain (but requiring no dangling bonds). Antiphase domains could easily explain the streaking in the  $\{\frac{1}{2}\frac{1}{2}\}$  spots.

It is worth considering a second model that satisfies valency considerations and has a Te coverage of 0.5 ML, namely, a structure in which the Ge surface is dimerized, and Te is adsorbed in every cave site (or long-bridge site). This geometry was favored by Leung *et al.* for the S/Ge(001)- $(2\times 1)$  system,<sup>41</sup> and considered by Yang *et al.* for Te/Si(001)- $(2\times 1)$ .<sup>11</sup> Upon closer inspection, it is unlikely that this structure could exist for the Te/Ge system: it is not possible to form this structure with reasonable values of bond lengths or bonding angles. If we consider the most liberal case, where the angle between the two Te-Ge bonds is allowed to be  $180^\circ$  and we assume an elongated Ge-Ge dimer bond length of 2.55 Å, the Te-Ge bondlength would be 2.73 Å, which is more than 7% longer than the sum of the covalent radii. Moreover, we now show that this model is inconsistent with our XSW data.

The (004) XSW data show that all Te atoms are located at the same adsorption height for the  $(\sqrt{2}\times\sqrt{2})R45^\circ$  structure. However, the reduced value of  $F_{022}(0.60\pm 0.02)$  indicates that not all Te are located at equivalent lateral positions within the surface unit cell. For our proposed model (Fig. 6), this simply means that there is an equal population of the two symmetrically equivalent domains of Te-Ge heterodimers. However, the cave-site model cannot accommodate inequivalent Te positions in any natural way, since Te adsorption occurs in that model at a high-symmetry site. As a final piece of evidence in support of the heterodimer structure, preliminary first-principles calculations of various arrangements of 0.5 ML Te/Ge(001) showed that the proposed structure has the lowest surface energy.<sup>42</sup>

We can now use the measured value of  $F_{022}$  to determine directly the lateral displacement of the Te atoms, and thus give a complete picture of the local geometry. The coherent fraction is given as the product of three factors

$$F_H = C a_H D_H, \quad (1)$$

where  $C$  is the fraction of atoms at ordered sites,  $D_H$  is the Debye-Waller factor discussed previously,  $a_H$  is a geometrical factor reflecting any inequivalence in the adsorption sites, and  $H$  is the diffraction vector. In this case,  $C\approx 1$  [based on

the (004) result] and we estimate  $D_{022} = 0.92 \pm 0.02$ .<sup>43</sup> The geometrical factor is a phase-weighted sum over the fluorescing species, and for the structure proposed in Fig. 6 will be given by

$$a_{022} = \left| \cos \frac{2\pi b}{d_{022}} \right|, \quad (2)$$

where  $b$  is the lateral displacement of the Te atom from the bridge site, and  $d_{022}$  is the interplanar spacing in the (022) direction (2.00 Å for Ge). From the measured value  $F_{022} = 0.60 \pm 0.02$ , this implies that  $a_{022} = 0.66 \pm 0.03$ . From this value, we can deduce that  $b = 0.73 \pm 0.01$  Å [where we exclude physically unreasonable inversions of Eq. (2)]. We have thus specified completely the Te atomic position within the  $(\sqrt{2} \times \sqrt{2})R45^\circ$  unit cell. Using these coordinates, we can infer that the length of the Te-Ge<sub>s</sub> backbond (from the Te to the last full layer of Ge) is  $2.61 \pm 0.03$  Å. Although we lack information to specify the Te-Ge<sub>a</sub> heterodimer bond length, we note that the measured Te position is consistent with very reasonable values of the bond lengths and angles. For example, our results are consistent with lengths of 2.59 and 2.45 Å, for the Te-Ge<sub>a</sub> dimer bond and Ge<sub>a</sub>-Ge<sub>s</sub> backbond, respectively, and a bonding angle between them of 109.3°. These are essentially identical to the sum of covalent radii and the tetrahedral angle.

Other than one LEED pattern,<sup>9</sup> no other data exist to our knowledge for Te adsorption on a Ge(001) substrate. However, there have been several published studies of SME of Ge/Si(001) using Te as a surfactant.<sup>8–12</sup> Some observations of these studies reinforce our conclusions; reciprocally, our conclusions help explain why Te is an effective surfactant for Ge/Si(001).

These studies all conducted growth of Ge on a Te-terminated Si(001) substrate. The Te precoverage was varied in some of the studies, and effective surfactant action was observed down to 0.1 ML.<sup>10</sup> With regard to the present paper, the most distinctive observation of those studies is the appearance of a  $(2 \times 2)$  (Refs. 9 and 12) or  $c(2 \times 2)$  (Ref. 11) LEED pattern. [The possible presence of  $(2 \times 1)$  spots from Group-IV-Group-IV dimers would make it difficult to distinguish between these patterns.] Typically, a  $(2 \times 2)$  pattern was reported to appear after significant Ge deposition with concomitant Te desorption. (Te desorbs from Ge at a lower temperature than it does from Si).<sup>20</sup> Thus, as the Te coverage was reduced, the  $(2 \times 2)$  or  $c(2 \times 2)$  pattern emerged. This is consistent with our observations that the  $c(2 \times 2)$  [i.e.,  $(\sqrt{2} \times \sqrt{2})R45^\circ$ ] superstructure has a lower ideal Te coverage.

The study of Bennett *et al.* carefully monitored the intensity of Si and Ge core-level peaks during Ge deposition. The shifted features corresponded to Si and Ge bound to one, two, three, or four Te atoms.<sup>12</sup> Referring to Figs. 5 and 6, we see that the 1-ML structure is dominated by Ge atoms bound to two Te atoms, while our  $\frac{1}{2}$  ML structural model predicts that Ge atoms will be coordinated to only one Te atom. Bennett *et al.* found that the Te/Si(001) starting surface predominantly contained Si coordinated to two Te atoms. Similarly, for the initial stages of Ge growth, the Ge was found to be coordinated to two Te atoms. It is presumed that, initially, Ge occupies only substitutional sites, and the local structure

is the same as our high-Te-coverage surface, i.e., the Te atoms bridge neighboring Ge atoms. Strikingly, they found that at latter stages of Ge deposition, the Te coverage was halved, and the population of two-Te-coordinated Ge atoms dwindled rapidly to zero. Of the Ge that was coordinated to Te, only Ge that was bound to exactly one Te atom remained in any significant numbers. This observation occurred at the same stage that the  $(2 \times 2)$  LEED pattern emerged. Bennett *et al.* interpreted these data as meaning that every other bridge site was empty, and the others were occupied by a Te atom in a local structure unchanged from the initial, high-coverage surface.<sup>12</sup> That arrangement would leave the Ge surface atoms unsatisfied, which seems unlikely. This structure, suggested by Bennett *et al.* for Te/Ge/Si(001), is excluded by our XSW data for Te/Ge(001), but the arrangement we propose is fully consistent with their photoemission data for high Ge coverages. Although one would not expect *a priori* that the identical structures would occur on Te/Ge(001) and Te/Ge/Si(001), the simplest interpretation is that, in both cases, Te exists in a bridge-bonded site at high coverages, and as a Te-Ge heterodimer at low coverages.

The SME studies also give some insight as to whether the driving force for the structural rearrangement reported here is due to the lower Te coverage after annealing, or if the rearrangement simply requires higher temperatures to be activated. The SME studies reported the emergence of  $(2 \times 2)$  spots after Ge growth at temperatures of 210–270 °C.<sup>9,11,12</sup> It seems clear, then, that the local Te coverage is the driving force, and the annealing in the present study served primarily to diminish the Te coverage.

The ability of Te to satisfy Ge dangling bonds in two different local structures with different local coverage helps to explain why Te is such an effective surfactant over a wide range of coverages. Evidently, Te can lower the surface energy (by eliminating dangling bonds) in one of two coordinations, depending on the local environment. During SME at high Te coverages, Ge can replace a Te atom at a substitutional site, while the Te atom segregates to another bridge site at the new surface.<sup>12</sup> If, on the other hand, Ge growth is carried out on a surface with Te-Ge heterodimers, it is reasonable to expect that a Ge monomer could replace the Te atom in the dimer. The Te atom could then take up either a bridge position above this Ge pair, or could migrate to a new position in either type of site. In future time-resolved XSW studies, we will attempt to infer the energy barrier of the suggested transition states by measuring the kinetics of this structural rearrangement.

## V. CONCLUSIONS

The surface structure of Te/Ge(001), while characterized by simple atomic adsorption sites, exhibits complex and subtle behavior. At high Te coverages, the adsorbates occupy simple bridge sites that reduce the local surface reconstruction to a  $(1 \times 1)$  geometry. The Te coverage saturates at near 1.0 ML. However, the compressive strain generated by the larger-atomic-radius adsorbate necessitates strain-relieving defects of missing Te rows. Also, the surface system exhibits a weak  $(2 \times 1)$  periodicity that we cannot presently explain. We conclude that this periodicity is associated

with the missing rows, but cannot exclude that it may be present in the local structure.

At lower Te coverages, an adsorption site unanticipated for a Group-VI/Group-IV(001) interface is occupied. The Te adsorbate forms a heterodimer with a Ge atom, thereby satisfying all surface dangling bonds with close to only 0.5 ML Te coverage. Additionally, the interaction of the Te-Ge heterodimers causes the dimer units to arrange themselves on a  $(\sqrt{2} \times \sqrt{2})R45^\circ$  unit mesh. The observation that Te can occupy two fundamentally different sites, both satisfying all dangling bonds but with different local coverages, can help explain why Te is a particularly effective surfactant for SME of Ge on Si(001).

## ACKNOWLEDGMENTS

The authors gratefully acknowledge useful discussions with K. Evans-Lutterodt, and thank N. Takeuchi for sharing unpublished calculations. This work was supported by the U.S. Department of Energy under Contract No. W-31-109-ENG-38 to Argonne National Laboratory, Contract No. DE-AC02-98CH10886 to the National Synchrotron Light Source at Brookhaven National Laboratory, and by the National Science Foundation under Contract No. DMR-9632593, and under Contract No. DMR-9632472 to the MRC at Northwestern University.

\*Author to whom correspondence should be addressed. Electronic address: bedzyk@nwu.edu

<sup>1</sup>M. Copel, M. C. Reuter, E. Kaxiras, and R. M. Tromp, *Phys. Rev. Lett.* **63**, 632 (1989).

<sup>2</sup>B. Voigtländer, A. Zinner, T. Weber, and H. P. Bonzel, *Phys. Rev. B* **51**, 7583 (1995).

<sup>3</sup>H. J. Osten, J. Klatt, G. Lippert, E. Bugiel, and S. Hinrich, *Appl. Phys. Lett.* **60**, 2522 (1992).

<sup>4</sup>P. F. Lyman and M. J. Bedzyk, *Appl. Phys. Lett.* **69**, 978 (1996).

<sup>5</sup>T. Weser, A. Bogen, B. Konrad, R. D. Schnell, C. A. Schug, and W. Steinmann, *Phys. Rev. B* **35**, 8184 (1987).

<sup>6</sup>S. A. Yoshikawa, J. Nogami, C. F. Quate, and P. Pianetta, *Surf. Sci.* **321**, L183 (1994).

<sup>7</sup>S. R. Burgess, B. C. C. Cowie, S. P. Wilks, P. R. Dunstan, C. J. Dunscombe, and R. H. Williams, *Appl. Surf. Sci.* **104/105**, 152 (1996).

<sup>8</sup>S. Higuchi and Y. Nakanishi, *Surf. Sci.* **254**, L465 (1991).

<sup>9</sup>S. Higuchi and Y. Nakanishi, *J. Appl. Phys.* **71**, 4277 (1992).

<sup>10</sup>H. J. Osten, J. Klatt, G. Lippert, E. Bugiel, and S. Higuchi, *J. Appl. Phys.* **74**, 2507 (1993).

<sup>11</sup>X. Yang, R. Cao, J. Terry, J. Wu, and P. Pianetta, in *Common Themes and Mechanisms of Epitaxial Growth*, edited by P. Foss, in MRS Symposia Proceeding No. 312 (Materials Research Society, Pittsburgh, 1993), p. 243; X. Yang, Ph.D. thesis, Stanford University, 1995.

<sup>12</sup>M. R. Bennett, C. J. Dunscombe, A. A. Cafolla, J. W. Cairns, J. E. Macdonald, and R. H. Williams, *Surf. Sci.* **380**, 178 (1997).

<sup>13</sup>M. W. Grant, M. A. Boshart, D. J. Dieleman, and L. E. Seiberling, *Surf. Sci.* **316**, L1088 (1994).

<sup>14</sup>J. Zegenhagen, *Surf. Sci. Rep.* **18**, 199 (1993).

<sup>15</sup>A. D. Johnson, C. Norris, J. W. M. Frenken, H. S. Derbyshire, J. E. Macdonald, R. G. Van Silfhout, and J. F. Van der Veen, *Phys. Rev. B* **44**, 1134 (1991).

<sup>16</sup>The dominant source of the coverage uncertainty is the uncertainty in the ion stopping power tables used to analyze the RBS spectra [J. F. Ziegler, J. P. Biersack, and U. Littmark, IBM Research Report RC9250, 1982 (unpublished)].

<sup>17</sup>K. Tamiya, T. Ohtani, Y. Takeda, T. Urano, and S. Hongo, *Surf. Sci.* **408**, 268 (1998).

<sup>18</sup>T. Ohtani, K. Tamiya, T. Urano, and S. Hongo, *Appl. Surf. Sci.* **130–132**, 112 (1998).

<sup>19</sup>It should also be noted that some workers have reported a “sharp ( $1 \times 1$ )” for adsorption of Te/Si(001). (See Ref. 11.) We have reproduced the streaky pattern, but have never seen a streak-free ( $1 \times 1$ ) for Te/Si(001).

<sup>20</sup>P. F. Lyman, D. L. Marasco, H. L. Hutchason, M. Keeffe, P. A.

Montano, and M. J. Bedzyk (unpublished).

<sup>21</sup>In previous direct and indirect measurements of various adsorbates (As, Sb, Bi) on Si surfaces, we consistently found values of  $\langle u_{004}^2 \rangle^{1/2}$  of 0.12–0.14 Å. For Bi/Si(001), a direct measurement revealed a value of  $0.13 \pm 0.015$  Å, which is used here. See P. F. Lyman, Y. Qian, T.-L. Lee, and M. J. Bedzyk, *Physica B* **221**, 426 (1996).

<sup>22</sup>It is expected that there will be an inward relaxation of the Ge-surface layer of 0.05–0.10 Å. For example, see P. F. Lyman, Y. Qian, and M. J. Bedzyk, *Surf. Sci.* **325**, L385 (1995). This assumption and the associated uncertainty are reflected in the cited bond length.

<sup>23</sup>L. Pauling and M. L. Huggins, *Z. Kristallogr.* **87**, 205 (1934).

<sup>24</sup>I. D. Nabitovich, Ya. I. Stetsiv, A. M. Andreiko, and R. Ya. Yurechko, *Kristallografiya* **20**, 1240 (1975) [*Sov. Phys. Crystallogr.* **20**, 758 (1975)].

<sup>25</sup>K. Hirota, K. Nagino, and G. Ohbayashi, *J. Appl. Phys.* **82**, 65 (1997).

<sup>26</sup>O. Uemura, N. Hayasaka, S. Tokairin, and T. Usuki, *J. Non-Cryst. Solids* **205–207**, 189 (1996).

<sup>27</sup>R. D. Bringans and M. A. Olmstead, *Phys. Rev. B* **39**, 12 985 (1989).

<sup>28</sup>E. Kaxiras, *Phys. Rev. B* **43**, 6824 (1991).

<sup>29</sup>P. Krüger and J. Pollmann, *Phys. Rev. B* **47**, 1898 (1993).

<sup>30</sup>Y.-J. Zhao, P.-L. Cao, and G. Lai, *J. Phys.: Condens. Matter* **10**, 7769 (1998).

<sup>31</sup>A. Papageorgopoulos, A. Corner, M. Kamaratos, and C. A. Papageorgopoulos, *Phys. Rev. B* **55**, 4435 (1997).

<sup>32</sup>J. Nogami, A. A. Baski, and C. F. Quate, *Appl. Phys. Lett.* **58**, 475 (1991).

<sup>33</sup>H. P. Noh, Ch. Park, D. Jeon, K. Cho, T. Hashizume, Y. Kuk, and T. Sakurai, *J. Vac. Sci. Technol. B* **12**, 2097 (1994).

<sup>34</sup>See, for example, M. Henzler, *Appl. Surf. Sci.* **11/12**, 450 (1982).

<sup>35</sup>W. Wegscheider and H. Cerva, *J. Vac. Sci. Technol. B* **11**, 1056 (1993).

<sup>36</sup>R. Sporcken, F. Malengreau, J. Ghijsen, R. Caudano, S. Sivananthan, J. P. Faurie, T. van Gemmeren, and R. L. Johnson, *Appl. Surf. Sci.* **123/124**, 462 (1998).

<sup>37</sup>D. J. Wallis, N. D. Browning, S. Sivananthan, P. D. Nellist, and S. J. Pennycook, *Appl. Phys. Lett.* **70**, 3113 (1997).

<sup>38</sup>J. F. Morar, U. O. Karlsson, R. I. G. Uhrberg, J. Kanski, P. O. Nilsson, and H. Qu, *Appl. Surf. Sci.* **41/42**, 312 (1989).

<sup>39</sup>M. Lohmeier, H. A. van der Vegt, R. G. van Silfhout, E. Vlieg, J. M. C. Thornton, J. E. Macdonald, and P. M. L. O. Scholte, *Surf. Sci.* **275**, 190 (1992).



- <sup>40</sup>W. A. Harrison, E. A. Kraut, J. R. Waldrop, and R. W. Grant, Phys. Rev. B **18**, 4402 (1978).
- <sup>41</sup>K. T. Leung, L. J. Terminello, Z. Hussain, X. S. Zhang, T. Hayashi, and D. A. Shirley, Phys. Rev. B **38**, 8241 (1988).
- <sup>42</sup>Noboru Takeuchi, (private communication).
- <sup>43</sup>This value again assumes the mean-square-displacement  $\langle u_{022}^2 \rangle^{1/2}$  to be approximately  $0.13 \pm 0.02$  Å. Note, however, that values

of lateral mean-square displacements tend to be lower than perpendicular displacements due to greater in-plane coordination. Thus, this value of  $\langle u_{022}^2 \rangle^{1/2}$  should be considered to be an upper bound and therefore the derived value of the Te atom shift  $b$  is an upper bound. The lower bound, which occurs for  $\langle u_{022}^2 \rangle^{1/2} = 0$ , is  $b = 0.71$  Å.